Short Papers

Differential-Flatness-Based Planning and Control of a Wheeled Mobile Manipulator—Theory and Experiment

Chin Pei Tang, Patrick T. Miller, Venkat N. Krovi, Ji-Chul Ryu, and Sunil K. Agrawal

***Abstract*—This paper presents a differential-flatness-based integrated point-to-point trajectory planning and control method for a class of nonholonomic wheeled mobile manipulator (WMM). We demonstrate that its kinematic model possesses a feedback-linearizable description due to the flatness property, which allows for full-state controllability. Trajectory planning can then be simplified and achieved by polynomial fitting method in the flat output space to satisfy the terminal conditions, while control design reduces to a pole-placement problem for a linear system. The method is then deployed on our custom-constructed WMM hardware to evaluate its effectiveness and to highlight various aspects of the hardware implementation.**

***Index Terms*—Differential flatness, integrated trajectory planning and control, nonholonomic system, wheeled mobile manipulator (WMM).**

I. Introduction

Autonomous or semiautonomous robotic systems have proven very useful in extending the reach and capabilities of humans in numerous manipulation and remote interaction tasks. The archetypal fixed-base robotic manipulator possesses considerable manipulation capabilities but limited workspace. Mounting such manipulator on mobile base creates the so-called mobile manipulator configuration with benefits including extended workspace, improved disturbance rejection capability, and reconfigurability. Numerous applications, ranging from advanced highway maintenance [1] to remote rescue mission [2] to cooperative payload transport [3] have capitalized on this merger of mobility with manipulation.

In this paper, we focus on the wheeled mobile manipulator (WMM) system formed by mounting a multi-degree-of-freedom manipulator on a wheeled mobile robot (WMR). While the conventional disc wheels are popular due to its robust physical construction, ease of addition to platforms, and ease of operation, the kinematics of rolling contact creates nonholonomic constraints and the resulting class of nonholonomic WMM requires special treatment [4]. We present a differential flatness-based integrated point-to-point planning and control method for the WMM and its experimental validation.

To succinctly summarize the differential-flatness approach [5], the states and inputs can be parameterized by a finite set of independent variables called the flat outputs, and their (time) derivatives. Such parameterization establishes a one-to-one mapping from the states and the inputs to the flat outputs. Since the number of flat outputs is equal to the number of control inputs, this allows the full-state controllability of the system. Perhaps more importantly, the system of governing ordinary differential equations can be transformed into a set of algebraic equations, which are generally simpler to solve. A *constraint-satisfying* desired trajectory can now be planned using a variety of interpolating functions, including polynomials of appropriate order, to match the constraint conditions in the flat output space. In addition, exponential stabilizing controllers can be developed since the system has the representation of a chain of integrators in the flat output space. Thus, these aspects facilitate a unified treatment of both the trajectory planning and control problems within a common framework.

Several *representative* methods for controlling a WMM have been reported in the literature. Seraji [6] proposed a unified Jacobian-based resolved rate control method by concatenating the Jacobians of the WMR and the manipulator subsystems. Bayle *et al.* [7] extended such redundancy resolution method by incorporating the idea of "preferred configuration" in the manipulability context similar to [8]. Unfortunately, these works focus on only simulation-based kinematic performance evaluation, assuming the availability of good rate controlled actuators, without an actual hardware implementation. White *et al.* [4] experimented within a novel dynamically consistent redundancy resolution method that prioritizes the end-effector tracking task while secondarily achieving WMR base tracking.

However, it is important to remember that Yamamoto and Yun [8] showed that a WMM system is not input-state linearizable by static-state feedback, but is input–output linearizable by appropriate selection of output coordinates. In fact, all of these approaches are not able to achieve point-to-point control on the full states of the system, but only looking at the end-point control and (potentially) uncontrollable internal dynamics, which is suboptimal. In this paper, we first show formally that by choosing the appropriate flat outputs, the system can be dynamically feedback-linearized (with the notion of prolongation in the differential-flatness context) to achieve full-state controllability.

Second, while differential-flatness approach offers an elegant integrated framework to simplify the motion planning/control problems [5], [9], [10], the literature beyond simulation-based verification is scarce. Hardware implementation can pose unforeseen challenges that can go undetected at the theoretical development or simulation stages. For instance, many commercially available robotic system provides only the joint rate-control input, but not the torque input, to the system. Hence, the second contribution of this paper comes from systematic and careful performance evaluation of controller deployment on experimental hardware, while ensuring compatibility with the rate-controlled actuators.

Manuscript received March 29, 2010; revised June 21, 2010; accepted July 31, 2010. Recommended by Technical Editor A. Menciassi. This work was supported in part by a National Science Foundation CAREER Award under Grant IIS-0347653. This paper was presented in part at the 2008 ASME Dynamic Systems and Control Conference, Ann Arbor, Michigan, October 20–22.

C. P. Tang is with the Erik Jonsson School of Engineering and Computer Science, University of Texas at Dallas, Richardson, TX 75080 USA (e-mail: chinpei@utdallas.edu).

P. T. Miller is with Calspan Corporation, Buffalo, NY 14225 USA (e-mail: patrickmiller@ieee.org).

V. N. Krovi is with the Department of Mechanical and Aerospace Engineering, State University of New York at Buffalo, Buffalo, NY 14260 USA (e-mail: vkrovi@buffalo.edu).

J.-C. Ryu and S. K. Agrawal are with the Department of Mechanical Engineering, University of Delaware, Newark, DE 19716 USA (e-mail: jcryu@udel.edu; agrawal@udel.edu).

Color versions of one or more of the figures in this paper are available online at http://ieeexplore.ieee.org.

Digital Object Identifier 10.1109/TMECH.2010.2066282

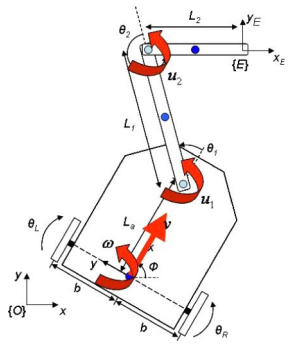

Fig. 1. Schematic of the WMM under consideration. The states are $[x, y, \varphi, \theta_1, \theta_2]^T$, the inputs are $[v, \omega, u_1, u_2]^T$, and the flat outputs are chosen to be $[x, y, \theta_1, \theta_2]^T$.

II. Differential Flatness-Based Planning and Control

A. Differential Flatness in WMM Model

Referring to Fig. 1, the WMM under consideration consists of a WMR base mounted with a planar two-link manipulator with generalized coordinates $\mathbf{q}^T = [\mathbf{q}_B^T, \mathbf{q}_M^T] = [x, y, \varphi, \theta_1, \theta_2]$. $\mathbf{q}_B^T = [x, y, \varphi]$ describes the configuration of the WMR, and $\mathbf{q}_M^T = [\theta_1, \theta_2]$ describes the joint configuration of the manipulator. (x, y) is the Cartesian position of the center of the axle of the WMR, φ is the orientation of the WMR, and θ_1, θ_2 are the relative angles that parameterize the first and second links of the mounted manipulator. The kinematics of the WMR including the nonholonomic constraints can be described as

$$\underbrace{\begin{bmatrix} \dot{x} \\ \dot{y} \\ \dot{\varphi} \end{bmatrix}}_{\dot{\mathbf{q}}_B} = \underbrace{\begin{bmatrix} \cos\varphi & 0 \\ \sin\varphi & 0 \\ 0 & 1 \end{bmatrix}}_{\mathbf{J}_B} \underbrace{\begin{bmatrix} v \\ \omega \end{bmatrix}}_{\mathbf{u}_B} \tag{1}$$

where v and ω are, respectively, the forward and angular velocities inputs. The extended WMM model can then be written as

$$\begin{bmatrix} \dot{\mathbf{q}}_B \\ \dot{\mathbf{q}}_M \end{bmatrix} = \begin{bmatrix} \mathbf{J}_B & \mathbf{0}_2 \\ \mathbf{0}_2 & \mathbf{I}_2 \end{bmatrix} \begin{bmatrix} \mathbf{u}_B \\ \mathbf{u}_M \end{bmatrix} \tag{2}$$

where $\mathbf{u}_M^T = [u_1, u_2]$ are the joint velocity inputs to the individual manipulator joints, $\mathbf{0}_2$ and $\mathbf{I}_2$ are, respectively, 2×2 zero and identity matrices.

We first show that (1) cannot be statically feedback linearized. Define the flat outputs

$$\mathbf{F}_B^T = [F_1, F_2] = [x, y]. \tag{3}$$

By differentiating (3) with respect to time, and noting that $\dot{x} = v\cos\varphi$ and $\dot{y} = v\sin\varphi$

$$\dot{\mathbf{F}}_B = \begin{bmatrix} \dot{F}_1 \\ \dot{F}_2 \end{bmatrix} = \begin{bmatrix} \dot{x} \\ \dot{y} \end{bmatrix} = \begin{bmatrix} \cos\varphi & 0 \\ \sin\varphi & 0 \end{bmatrix} \begin{bmatrix} v \\ \omega \end{bmatrix}. \tag{4}$$

The mapping between the inputs and the flat outputs turns out to be singular. This problem can be addressed by introducing the *input prolongation* of v (extending v as a state) [5], and extending the system to

$$\dot{x} = v\cos\varphi,\ \dot{y} = v\sin\varphi,\ \dot{v} = \eta,\ \dot{\varphi} = \omega \tag{5}$$

where η is the new (time derivative of the forward velocity) input to the system. By taking the double time derivatives of the flat outputs

$$\ddot{\mathbf{F}}_B = \begin{bmatrix} \ddot{F}_1 \\ \ddot{F}_2 \end{bmatrix} = \begin{bmatrix} \ddot{x} \\ \ddot{y} \end{bmatrix} = \begin{bmatrix} \cos\varphi & -v\sin\varphi \\ \sin\varphi & v\cos\phi \end{bmatrix} \begin{bmatrix} \eta \\ \omega \end{bmatrix}. \tag{6}$$

Effectively, the modified inputs to the system are η and ω. For the manipulator, we can choose the flat outputs to be

$$\mathbf{F}_M^T = [F_3, F_4] = \mathbf{q}_M^T = [\theta_1, \theta_2]. \tag{7}$$

Using the definition of differential flatness in the Appendix, we can then state the following:

Proposition 2.1: WMM model in (2) is differentially flat.

Proof: We choose the complete set of flat outputs $\mathbf{F}^T = [\mathbf{F}_B^T, \mathbf{F}_M^T]$ defined in (3) and (7). We can show that the states and the inputs of the system can be completely expressed by the flat outputs (and their time derivatives) as

$$\begin{aligned} &x = F_1, y = F_2, \varphi = \tan^{-1}\left(\frac{\dot{F}_2}{\dot{F}_1}\right) \\ &v = \sqrt{\dot{F}_1^2 + \dot{F}_2^2},\ \omega = \frac{\dot{F}_1\ddot{F}_2 - \ddot{F}_1\dot{F}_2}{\dot{F}_1^2 + \dot{F}_2^2},\ \eta = \frac{\dot{F}_1\ddot{F}_1 + \dot{F}_2\ddot{F}_2}{\sqrt{\dot{F}_1^2 + \dot{F}_2^2}} \\ &\theta_1 = F_3,\ \theta_2 = F_4,\ \dot{\theta}_1 = u_1 = \dot{F}_3,\ \dot{\theta}_2 = u_2 = \dot{F}_4. \end{aligned} \tag{8}$$

Conversely, the flat outputs can also be expressed completely by the states and the inputs (and their time derivatives) as

$$\begin{aligned} F_1 &= x, F_2 = y, F_3 = \theta_1, F_4 = \theta_2 \\ \dot{F}_1 &= \dot{x} = v\cos\varphi, \dot{F}_2 = \dot{y} = v\sin\varphi \\ \ddot{F}_1 &= \dot{v}\cos\varphi - v\dot{\varphi}\sin\varphi = \eta\cos\varphi - v\dot{\varphi}\sin\varphi \\ \ddot{F}_2 &= \dot{v}\sin\varphi - v\dot{\phi}\cos\varphi = \eta\sin\varphi - v\dot{\phi}\cos\varphi. \end{aligned} \tag{9}$$

Hence, the system in (2) is differentially flat. ■

The diffeomorphic relationship in (8) and (9) establishes the one-to-one mapping between the flat output space and the state space, which allows the full-state controllability in the flat output space. The principal benefits are in the significant simplifications that result for the planning and control problem, as illustrated in the following.

B. Differential Flatness-Based Controller

We now pursue the development of a controller, for which the system in (9) can be linearized using the following change of inputs:

$$\ddot{F}_1 = \xi_1, \ddot{F}_2 = \xi_2, \dot{F}_3 = \xi_3, \dot{F}_4 = \xi_4. \tag{10}$$

Given the desired trajectories of the flat outputs $F_i^d(t)$, $i = 1, \ldots, 4$ (which we will plan later), the control laws to the new inputs can then be defined as

$$\begin{aligned} \xi_1 &= \ddot{F}_1^d + p_1\dot{e}_1 + p_2 e_1, \quad \xi_3 = \dot{F}_3^d + r_1 e_3 \\ \xi_2 &= \ddot{F}_2^d + q_1\dot{e}_1 + q_2 e_2, \quad \xi_4 = \dot{F}_4^d + s_1 e_4 \end{aligned} \tag{11}$$

where $p_1, p_2, q_1, q_2, r_1, s_1$ are the control gains, and $e_i = F_i^d - F_i$. The corresponding linearized error system can then be written as

$$\begin{aligned} \ddot{e}_1 + p_1\dot{e}_1 + p_2 e_1 = 0, \quad \dot{e}_3 + r_1 e_3 = 0 \\ \ddot{e}_2 + q_1\dot{e}_2 + q_2 e_2 = 0, \quad \dot{e}_4 + s_1 e_4 = 0. \end{aligned} \tag{12}$$

The control gains can then be chosen such that all the roots of the characteristic equations of the closed-loop error dynamics in (12) lie in the left half-plane of the complex plane to ensure exponential stability.

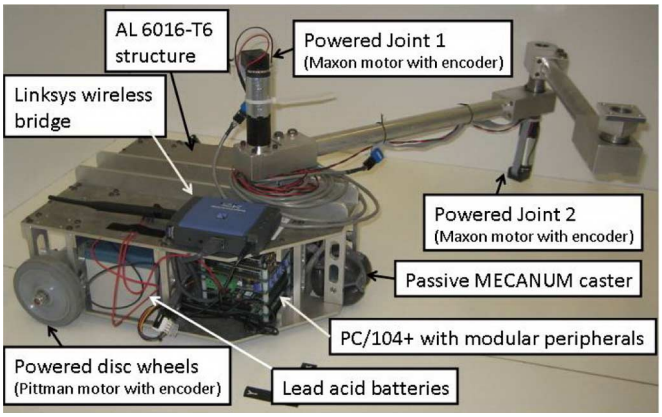

Fig. 2. Experimental electromechanical prototype of the WMM.

C. Integrated Trajectory Planning

We now present a simple polynomial-based trajectory planning for a given set of terminal conditions. Given the time interval $t \in [0, T]$ and the terminal conditions of the states

$$x(0), y(0), \varphi(0), v(0), \eta(0), \omega(0), \theta_1(0), \theta_2(0), \dot{\theta}_1(0), \dot{\theta}_2(0)$$
$$x(T), y(T), \varphi(T), v(T), \eta(T), \omega(T), \theta_1(T), \theta_2(T), \dot{\theta}_1(T), \dot{\theta}_2(T).$$

They can be transformed to the following corresponding terminal conditions in the flat outputs using (9):

$$F_1(0), \dot{F}_1(0), \ddot{F}_1(0), F_2(0), \dot{F}_2(0), \ddot{F}_2(0), F_3(0), \dot{F}_3(0), F_4(0), \dot{F}_4(0)$$
$$F_1(T), \dot{F}_1(T), \ddot{F}_1(T), F_2(T), \dot{F}_2(T), \ddot{F}_2(T), F_3(T), \dot{F}_3(T), F_4(T), \dot{F}_4(T). \quad (13)$$

Arbitrary trajectories of $F_i(t)$ can be constructed in the flat output space, provided that the trajectories satisfy these terminal conditions. We can plan desired trajectories $F_i^d(t)$ in polynomial form as

$$\begin{aligned} F_1^d(t) &= a_5 t^5 + a_4 t^4 + a_3 t^3 + a_2 t^2 + a_1 t + a_0 \\ F_2^d(t) &= b_5 t^5 + b_4 t^4 + b_3 t^3 + b_2 t^2 + b_1 t + b_0 \\ F_3^d(t) &= c_3 t^3 + c_2 t^2 + c_1 t + c_0 \\ F_4^d(t) &= d_3 t^3 + d_2 t^2 + d_1 t + d_0. \end{aligned} \quad (14)$$

The coefficients of the polynomials, a_k, b_k, c_l, d_l, $k = 0, \ldots, 5$, $l = 0, \ldots, 3$, can be determined uniquely using the terminal conditions in (13).

III. Hardware Implementation

A. Hardware Platform and Experimentation

We custom-built an open-architecture WMM, shown in Fig. 2, from the viewpoint of flexibility offered over retrofitting an off-the-shelf WMR base with an off-the-shelf manipulator arm. We employ the staged hardware-in-the-loop methodology for rapid experimental verification of the real-time controllers on the electromechanical mobile manipulators prototype. The physical parameters of the system are tabulated in Table I.

The WMR base consists of two dc motor powered wheels and one passive MECANUM-type caster. Conventional disc-type rear wheels, powered by two higher torque rating geared motors from Pittman, are chosen because of the robust physical construction, the ability to actuate the heavy base, and the ease of operation in the presence of terrain irregularities. Optical encoders at the motors provide the encoder feedback and odometry information for the base platform. A passive MECANUM-type front caster was preferred over a conventional wheel casters to eliminate the constraints on the maneuverability. The mounted manipulator arm has two actuated revolute joints with axes of rotation parallel to each other and perpendicular to the mobile platform and the ground. The first joint can be placed anywhere along the midline on top frame of the platform. The lengths of the first and second links can be freely adjusted by changing the length of the connecting rod. The two joints are also equipped with Maxon dc geared motor with lower torque rating and instrumented with optical encoders that can also measure the joint rotations. Two different lead-acid batteries provide power supplies for the actuator systems and the electronic controllers.

TABLE I
Physical Parameters of the WMM

Parameters	Values
Half distance between the two wheels (b)	$0.182m$
Radii of the wheels (r)	$0.0508m$
Distance from the center of the wheel axle to the base of the manipulator (L_a)	$0.216m$
Length of Link 1 (L_1)	$0.508m$
Length of Link 2 (L_2)	$0.362m$
Mass of WMR	$17.25kg$
Mass of Link 1	$2.56kg$
Mass of Link 2	$1.07kg$

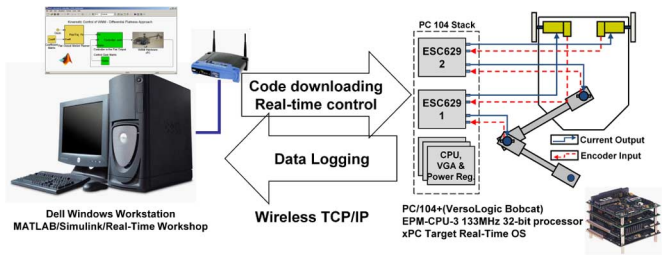

Fig. 3. MATLAB/xPC Target hardware-in-the-loop control framework.

TABLE II
Motor and ESC Parameters

	WMR (θ_R, θ_L)	Manipulator (θ_1, θ_2)
Motor Model	Pittman	Maxon
Actuator Speed Limit	$7.4rad/s$	$5.6rad/s$
ESC629 Control Gains, $[K_P, K_D, K_I]$	$[5,400, 5]$	$[100,600, 6]$
ESC629 Integration Limit	400	400

Referring to Fig. 3, a PC/104 system loaded with xPC Target Real-Time Operating System serves as the embedded controller of the electromechanical system, operating at the sampling rate of 5 ms. A PC104+ embedded computer (VersaLogic EPM-CPU-3 133MHz 32-bit processor with standard PC I/O and 10/100 Ethernet) is used to do all the on-board high-level processing, control, and communication processes for the system. Wireless communication is accomplished with a standard wireless Ethernet bridge. The host computer runs MATLAB/Simulink/Real Time Workshop, a convenient graphical interface supporting block-diagram-based control design, code compilation, and host/target communication. Compiled C code as well as real-time data can be transferred back and forth between the host and target computer using the TCP/IP connection. Code downloaded to the embedded controller can directly access the local hardware. This provides the ability to test the individual hardware components of the system

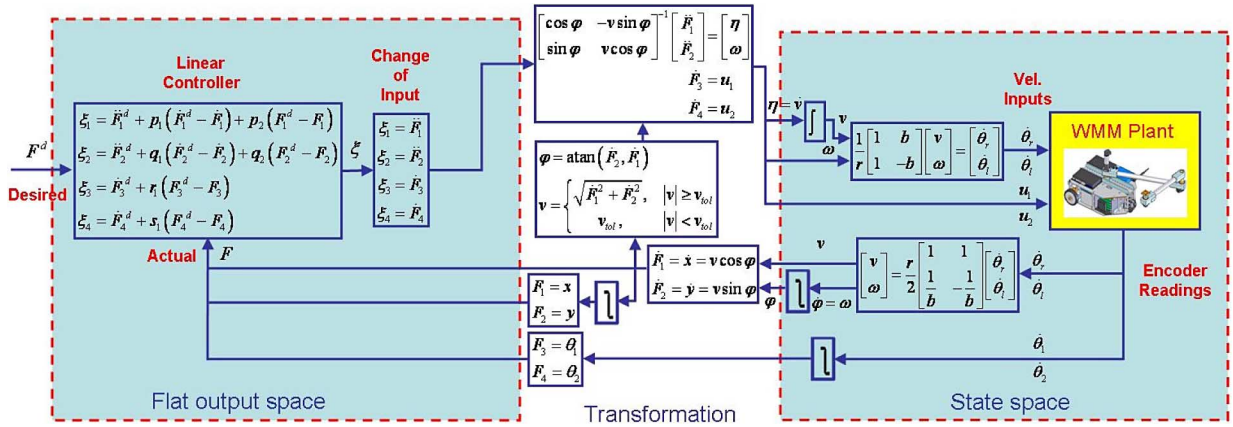

Fig. 4. Differential flatness-based control implementation framework for a WMM.

(i.e., individual motors and encoders) or the entire unit at once, using a staged hardware-in-the-loop methodology that we implemented.

The motion control system consists of four dc motors that are controlled by two ESC629, a 2-channel dc servo motor interface board with an on-board incremental encoder input and proportional-integral-derivative gain tunings—see Table II for the parameter details. For optimal power operation, the two ESC629 are configured such that each controlling one higher torque and one lower torque motor. The low-level C-style S-function codes were custom written to interface the ESC629 to the embedded controller and afford us board-level access to fine tune control parameters. Finally, finite-impulse-response-filter-based discrete-time differentiator was implemented to obtain the velocity of the motors based on the (positional) encoder data.

B. Control Implementation Details

Fig. 4 shows the block diagram that summarizes the complete control implementation in our system. To compute the original input to the physical system, we first substitute (11) into (10). The required control inputs to the manipulator u_1, u_2 can be calculated from (8). For the inputs to the WMR, we invert (6) to obtain η and ω, where the values of v and φ are obtained from the transformations of the quantities from the sensor readings. However, since the inversion of (6) is singular if $v = 0$, we set $v = v_{\rm tol}$ when $|v| \leq v_{\rm tol}$, where $v_{\rm tol}$ is a small velocity value (we take 0.01 m/s in our case). The corresponding input v can then be computed by integrating η. Note that since the value of v is always positive in our case, this approach can be directly applied to special class of mobile robots that can perform only forward motion. Finally, the corresponding right and left wheel velocity inputs ($\dot{\theta}_R$ and $\dot{\theta}_L$, respectively) can be obtained from the v and ω using the equations shown in the block diagram. For the sensor-reading feedback, the quantities v and ω can also be computed from the wheel-velocity readings. However, it is worth noting that the feedback does not suffer from the singular condition when $v = 0$, hence, the system is able to initialize even when the robot is initially at rest. Furthermore, there is no acceleration information required during the full control operation.

IV. Experimental Results

The proposed method has been thoroughly evaluated in both real-time simulations and experiments [11]. In this section, we show the representative case study to demonstrate the effectiveness of the proposed method, and highlight some of the consideration during the implementation. The method was first evaluated within the Real-Time Windows Target simulation framework to ensure that it is computationally feasible. We then converted the same code for the xPC Target-based implementation on the hardware platform as described previously.

We selected the gains as $p_1 = 2$, $p_2 = 1$, $q_1 = 6$, $q_2 = 9$, $r_1 = 3$, and $s_1 = 3$ such that the error transients are overdamped. The presented experimental case study was run under the following conditions with $T = 15$ s:

$$x^d(0) = 0.0m, y^d(0) = 0.0m, \varphi^d(0) = 0^\circ, \theta_1^d(0) = 0^\circ, \theta_2^d(0) = 0^\circ$$
$$x^d(T) = 1.5m, y^d(T) = 0.5m, \varphi^d(T) = 0^\circ, \theta_1^d(T) = 45^\circ, \theta_2^d(T) = 90^\circ.$$

Figs. 5–7 depict both the real-time simulation and experimental results.[1] Fig. 5 shows the state trajectories of the motion of the WMM computed from the encoder readings, and superimposed with the desired/simulated results. Fig. 6 shows the screenshots of the corresponding WMM motion.

While the tracking of the states is achieved closely, the resulting input profile is reasonably sensitive to the selection of the control gains. Furthermore, due to the existence of velocity saturation of each actuator, we cannot select very high gain that requires high input profiles—a fact that is often ignored by many analyses in the literature. Hence, we plot the angular velocity inputs of each actuator in Fig. 7 for careful evaluation. It can be seen that the required actual input profiles follow quite closely to the simulated input profiles. The initial fluctuations of all the input profiles are mainly due to the input effort of the actuators to account for the system mass and friction.

Finally, notice in the third subplot of Fig. 5 and the final configuration shown in Fig. 6, the final WMR orientation has a small error. This is because the quantity φ is not a directly measured quantity (not a flat output), and it is very sensitive to the odometry (velocity) data from the wheels. Furthermore, the selection of the gain for the second flat output, namely, $F_2 = y$, is also sensitive due to the existence of the nonholonomic constraints in the y-direction. If the gains are selected to be too high, it requires very high v and ω inputs (and the corresponding high-input wheel velocities $\dot{\theta}_R$ and $\dot{\theta}_L$), which saturates the hardware. If the gains are selected to be too low, the desired φ might not be achieved accurately. This is another issue that has to be carefully tradeoff during hardware implementation.

V. Conclusion

In this paper, we presented the differential flatness-based integrated planning and control framework for a class of nonholonomic WMM

[1]The video of the experiment can be found at http://www.youtube.com/watch?v=nGXgJ0w2dtE.

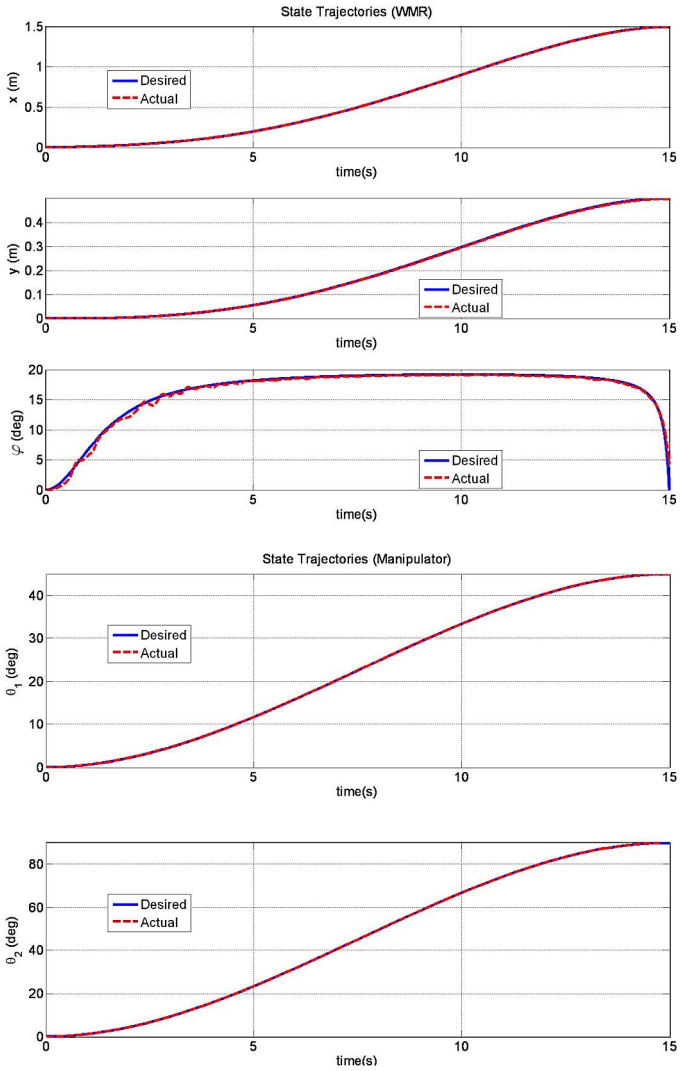

Fig. 5. Simulation and experimental results of the state trajectories $x(t), y(t), \varphi(t), \theta_1(t), \theta_2(t)$.

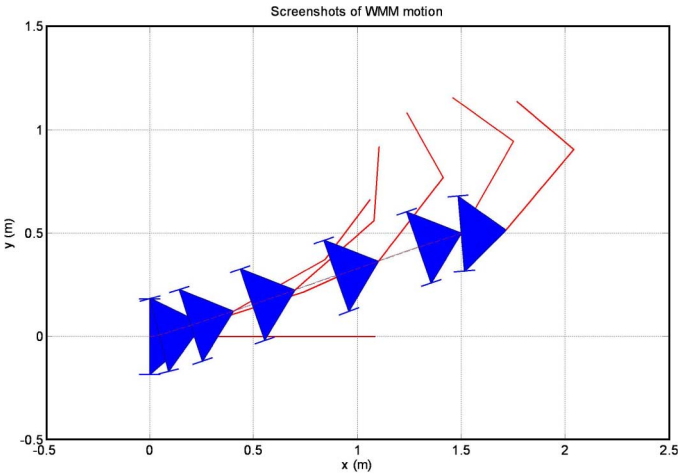

Fig. 6. Screenshots of the experimental WMM motion (from left to right, and plotting at the frame rate of 1 frame per 2.5 s).

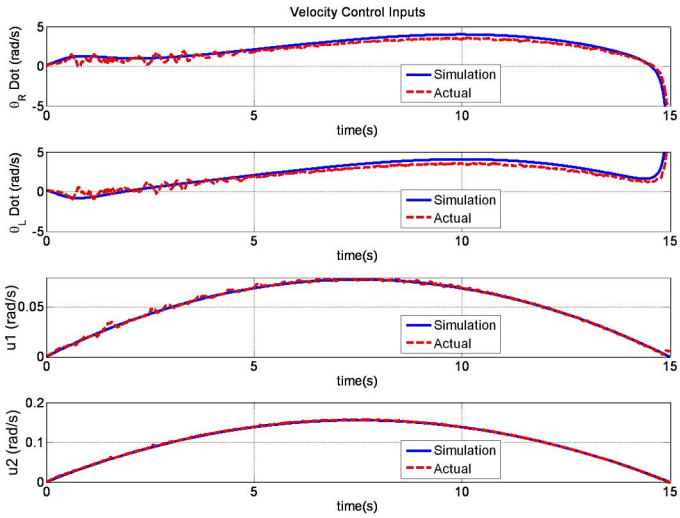

Fig. 7. Angular velocity input to each actuator $\dot{\theta}_R(t), \dot{\theta}_L(t), u_1(t), u_2(t)$.

to achieve full-state controllability. We first showed that the kinematic model under consideration is differentially flat by establishing the one-to-one mapping between the states of the system and the corresponding flat output space. The planning problem then reduced to a curve fitting problem, i.e., using polynomials of appropriate order to satisfy the specified terminal conditions in the flat output space. The corresponding control problem simplified to a linear system pole-placement problem with guaranteed stability. Finally, we demonstrated the applicability of the framework on a custom-made electromechanical WMM platform, and highlighted some of the implementation details. We are currently also evaluating a similar planning/control method for a dynamic/torque-controlled WMM.

APPENDIX

We here review the definition of a differentially flat system [5]. Given a set of ordinary differential equations that model a system. Let $\mathbf{q}$ be the vector of states and $\mathbf{u}$ be the vector of inputs. The system is said to be *differentially flat* if we can define a vector of *flat outputs* $\mathbf{F}$ such that the states and the inputs can be completely expressed by this set of flat outputs and its time derivatives as: $\mathbf{q} = \mathbf{f}_q(\mathbf{F}, \dot{\mathbf{F}}, \ldots, \mathbf{F}^{(m)})$, $\mathbf{u} = \mathbf{f}_u(\mathbf{F}, \dot{\mathbf{F}}, \ldots, \mathbf{F}^{(n)})$, and this set of flat outputs can also be completely expressed by the states and the inputs, and their time derivatives, as: $\mathbf{F} = \mathbf{g}_F(\mathbf{q}, \dot{\mathbf{q}}, \ldots, \mathbf{q}^{(m)}, \mathbf{u}, \dot{\mathbf{u}}, \ldots, \mathbf{u}^{(n)})$.

REFERENCES

[1] J. F. Gardner and S. A. Velinsky, "Kinematics of mobile manipulators and implications for design," *J. Robot. Syst.*, vol. 17, no. 6, pp. 309–320, May 2000.

[2] D. Ryu, J.-B. Song, C. Cho, S. Kang, and M. Kim, "Development of a six DOF haptic master for teleoperation of a mobile manipulator," *Mechatronics*, vol. 20, no. 2, pp. 181–191, Mar. 2010.

[3] C. P. Tang, R. M. Bhatt, M. Abou-Samah, and V. N. Krovi, "Screw-theoretic analysis framework for payload transport by mobile manipulator collectives," *IEEE/ASME Trans. Mechatronics*, vol. 11, no. 2, pp. 169–178, Apr. 2006.

[4] G. D. White, R. M. Bhatt, C. P. Tang, and V. N. Krovi, "Experimental evaluation of dynamic redundancy resolution in a nonholonomic wheeled mobile manipulator," *IEEE/ASME Trans. Mechatronics*, vol. 14, no. 3, pp. 349–357, Jun. 2009.

[5] H. Sira-Ramirez and S. K. Agrawal, *Differentially Flat Systems*. New York: Marcel Dekker, 2004.

[6] H. Seraji, "A unified approach to motion control of mobile manipulators," *Int. J. Robot. Res.*, vol. 17, no. 2, pp. 107–118, 1998.

[7] B. Bayle, M. Renaud, and J.-Y. Fourquet, "Nonholonomic mobile manipulators: Kinematics, velocities and redundancies," *J. Intell. Robot. Syst.*, vol. 36, pp. 45–63, 2003.

[8] Y. Yamamoto and X. Yun, "Coordinating locomotion and manipulation of a mobile manipulator," *IEEE Trans. Autom. Control*, vol. 39, no. 6, pp. 1326–1332, Jun. 1994.

[9] M. Fliess, J. Levine, P. Martin, and P. Rouchon, "Flatness and defect of non-linear systems: Introductory theory and examples," *Int. J. Control*, vol. 61, no. 6, pp. 1327–1361, 1995.

[10] J.-C. Ryu and S. K. Agrawal, "Planning and control of under-actuated mobile manipulators using differential flatness," *Auton. Robots*, vol. 29, no. 1, pp. 35–52, Jan. 2010.

[11] C. P. Tang, P. T. Miller, V. N. Krovi, J.-C. Ryu, and S. K. Agrawal, "Kinematic control of a nonholonomic wheeled mobile manipulator—A differential flatness approach," presented at the ASME Dyn. Syst. Control Conf., Ann Arbor, Michigan, Oct. 2008.